Journal of Materials Chemistry B

Accepted Manuscript

ROYAL SOCIETY OF CHEMISTRY

www.rsc.org/materialsB

Journal of Materials Chemistry B

Dynamic Article Links►

Cite this: DOI: 10.1039/c0xx00000x

ARTICLE TYPE

www.rsc.org/xxxxxx

Low temperature synthesis of phosphorous and nitrogen co-doped yellow fluorescent carbon dots for sensors and bioimaging†

Xiaojuan Gong,‡[a] Wenjing Lu,‡[a] Yang Liu,[a] Zengbo Li,[a] Shaomin Shuang,[a] Chuan Dong[a*] and Martin M.F. Choi[b1**]

Received (in XXX, XXX) XthXXXXXXXXX 20XX, Accepted Xth XXXXXXXXX 20XX
DOI: 10.1039/

Phosphorous and nitrogen co-doped carbon dots (P,N-CD) with satisfactory quantum yield have been prepared through one-step acidic oxidation of pumpkin by H_3PO_4 at low temperature (90°C). The as-prepared P,N-CD is relatively monodisperse with a narrow size distribution. The P,N-CD displays a remarkable emission enhancement in the yellow fluorescence region (λ_{em} = 550 nm) when the pH is increased from 1.5 to 7.4. The pK_a of P,N-CD was found to be 4.17 and it shows linear response to physiological range of pH 4.7–7.4, which is valuable for near-neutral cytosolic pH research. It is observed that P,N-CD is a superior fluorescent bioimaging agent in animals and cells thanks to its excellent solubility and ultra-low toxicity. In addition, P,N-CD displays a notably large Stokes shift of 125 nm, good reversibility and could effectively avoid the influence of autofluorescence in biological systems. The confocal fluorescent microscopic images of subcellular distribution and the detection of pH in MCF-7 cells were achieved successfully, suggesting that P,N-CD has excellent cell membrane permeability and is further applied successfully to monitor pH fluctuations in live cells with negligible autofluorescence.

Introduction

Carbon dots (CD), a rising star of fluorescent nanomaterials, with high aqueous solubility, tuneable photoluminescence (PL), robust chemical inertness, easy functionalisation, low environmental hazard, and excellent biocompatibility,[1,2] have attracted tremendous attention due to their promising applications in bioimaging,[3-5] drug delivery,[6] ink,[7-9] sensors,[10-13] optoelectronics,[14-16] and photocatalysis.[17-19] To date, there have been remarkable advances in research on the synthesis of CD and their synthesis methods can be divided into two major types: chemical and physical methods.[2] Chemical methods consist of electrochemical,[20,21] thermal treatment,[22] hydrothermal or acidic oxidation,[23-25] microwave,[26-28] ultrasonic,[29,30] and cage-opening of fullerene.[31] Physical methods include arc discharge,[32] laser ablation,[33,34] and plasma treatment.[35] Out of these methods, acidic oxidation has been proved to be an effective and convenient way for synthesis of CD with sufficient fluorescence quantum yield (Φ_s) without elaborate apparatus.

Currently, with the rapid development of synthesis methods, functionalised or doped CD has become a hot topic since functionalising or doping heteroatoms into CD can effectively tune the intrinsic properties of CD. Kwon *et al.*[36] synthesised sulfur-incorporated CD with a very strong long-wavelength absorption band. Dong *et al.*[37] devised polyamine functionalised CD with high Φ_s by carbonising citric acid with branched polyethylenimine in one-step procedure. Zheng *et al.*[38] fabricated reduced state CD via sodium borohydride. The Φ_s of the reduced state CD could increase from 2 to 24% and the maximum PL wavelength is shifted from 520 to 450 nm. Zhang *et al.*[39] prepared nitrogen (N)-doped CD with tuneable luminescence by adjusting the N contents. Similarly, Qian *et al.*[40] improved the Φ_s of CD by incorporating N atoms and speculated that the fluorescence enhancement is originated from the polyaromatic structures induced by the doped N. To our knowledge, synthesis of phosphorous and nitrogen co-doped CD emitting yellow fluorescent with a narrow size distribution has rarely been reported. Chandra *et al.*[41] synthesised phosphate functionalised fluorescent carbon nanoparticles (CNPs) by microwave irradiation. The size distribution of the as-prepared CNPs was 3–10 nm and they showed a PL at 454.5 nm. Unfortunately, the size distribution and PL properties of these CNPs were not well enough to apply in bioimaging directly. So they further functionalised them with organic dyes to improve the PL properties of CNPs. However, the development of fast and cost-effective ways to synthesise nontoxic phosphorous and nitrogen co-doped yellow fluorescent carbon dots (P,N-CD) from natural sources is still challenging.

Recently, there has been a trend to synthesise doped CD from natural biomass as they are inexpensive, inexhaustible and nontoxic. Several successful demonstrations were given to prepare nanomaterials using biomass materials which had many potential applications.[7,42-44] We are interested in developing convenient ways to synthesise P,N-CD from environmentally friendly materials and simple apparatus. As we all know, pumpkin abounds with carbon, nitrogen, oxygen, phosphorus, sulfur, and hydrogen elements owing to the existence of carbohydrate, protein, lipid, and glutathione. Thus, we anticipate that this natural material should be a promising precursor for

synthesising P,N-CD.

Herein, for the first time, we report a more convenient, economical, and green preparative strategy to synthesise P,N-CD by an acidic oxidation of pumpkin at low temperature (90°C). Interestingly, we successfully obtained P,N-CD emitting yellow fluorescence without post surface passivation. In addition, the as-prepared P,N-CD is monodisperse with a relatively narrow size distribution and possesses favourable PL properties. In addition, their PL stability under various external conditions such as high ionic strength and xenon arc light irradiation has been studied. The as-synthesised P,N-CD have been successfully utilised to fluorescent sensing of pH. The biocompatibility of the P,N-CD was assessed and their potential applications in *in vitro* and *in vivo* bioimaging agent were explored. Finally, the obtained P,N-CD shows application in oestrogenic differentiation. Phosphates had been reported to play an important role in mineralised tissue development such as bone formation.[45] We anticipate that our P,N-CD could possibly function as an excellent supercapacitor as Lu *et al.*[46] have reported that P-rich microporous carbons prepared by a simple H_3PO_4 activation could possess an extraordinary supercapacitive property.

Experimental

Materials

Yellow pumpkin was purchased from a local market in Taiyuan, China. Concentrated phosphoric acid (H_3PO_4), sodium hydroxide (NaOH), potassium chloride (KCl), and sodium chloride (NaCl) were from Aldrich (Milwaukee, WI, USA). Dimethyl sulfoxide (DMSO), Dulbecco's modified Eagle's medium (DMEM), festal bovine serum (FBS), trypsin, ethylenediaminetetraacetic acid (EDTA), and 3-(4,5-dimethylthiazol-2-yl)-2,5-diphenyltetrazolium bromide (MTT) were purchased from Solarbio (Beijing, China). Other reagents were from Beijing Chemical Reagents Company (Beijing, China). All reagents of analytical reagent grade or above were used as received without further purification. All aqueous solutions were prepared with ultrapure water (≥ 18.25 MΩ·cm) from a Milli-Q Plus system (Millipore, Bedford, MA, USA).

Synthesis of phosphorous and nitrogen co-doped carbon dots

Pumpkin was washed, peeled and seeds were removed by a stainless steel knife. The peeled pumpkin was thinly sliced and kept at -20°C before use. To prepare P,N-CD, 2.0 g of freeze-dry pumpkin was dispersed in 5.0 mL of ultrapure water, and 10 mL of 85% H_3PO_4 was added. After sonication for 10 min, the solution was heated at 90°C for 60 min. The pH was neutralised with NaOH (1M). The crude product was dialysed against water 72 h (molecular weight cut-off, MWCO: 500–1000 Da) and then filtered. The final product was freeze-drying until further use.

Characterisation

The elemental analysis was conducted on an ElementarAnalysensystemevario EL cube elemental analyser (Hanau, Germany). Analyses were performed in triplicate and the average values were obtained. The transmission electron microscopic (TEM) images were acquired on a JEOL JEM-2100 transmission electron microscope (Tokyo, Japan) with an accelerating voltage of 300 kV. The Fourier transform infrared spectra (FTIR) were recorded on a Bruker Tensor II FTIR spectrometer (Bremen, Germany). The X-ray photoelectron spectra (XPS) were acquired on an AXIS ULTRA DLD X-ray photoelectron spectrometer (Kratos, Tokyo, Japan) with AlKα radiation operating at 1486.6 eV. Spectra were processed by Case XPS v.2.3.12 software using a peak-fitting routine with symmetrical Gaussian-Lorentzian functions. The UV-vis spectra were performed on a Varian Cary 300 Scan UV-vis absorption spectrophotometer at 200–600 nm. The PL spectra were recorded on an Edinburgh FLS 920 spectrofluorometer (Livingston, UK).

Fluorescence assay of pH

The detection of pH was performed in 10 mM phosphate buffer saline (PBS containing 150 mM NaCl) at various pHs. In a typical run, 100 µL of P,N-CD dispersion (2.0 mg/mL) was added into 1.90 mL of PBS at various pHs. The fluorescence emission spectra were recorded after 3 min at room temperature. The measurements were conducted in triplicate.

MTT assays and cell imaging

For the cell cytotoxicity test, human breast adenocarcinoma MCF-7 cells were first plated on a Costar® 96-well cell culture cluster and cultured at 37°C with 5.0% CO_2 in air for 3 h to adhere cells onto the surface. The well without cells and treatment with P,N-CD was taken as the zero sets. The medium was then changed with 200 µL of fresh DMEM supplemented with 10% FBS containing P,N-CD and the cells were allowed to grow for another 24 and 48 h, respectively. At least six parallel samples were performed in each group. Cells not treated with P,N-CD were taken as the controls. After adding 20 µL of 5.0 mg/mL MTT reagent into every well, the cells were further incubated for 4 h. The culture medium with MTT was removed and 150 µL of DMSO was added. The resulting mixture was shaken for *ca.* 10 min at room temperature. The optical density (OD) of the mixture was measured at 490 nm with a SunRise microplate reader (Tecan Austria GmbH, Grödig, Austria). The cell viability was estimated as: $Cell\ viability\ (\%) = (OD_{Treated}/OD_{Control}) \times 100\%$, where $OD_{Control}$ and $OD_{Treated}$ were obtained in the absence and presence of P,N-CD, respectively.

Human breast adenocarcinoma MCF-7 cells were cultured in DMEM supplemented with 10% FBS, and the cells were seeded in the culture dish at 37°C in a 5% CO_2 atmosphere for 48 h. Then the culture medium was removed and the cells were washed with PBS. P,N-CD dissolved in ultrapure water was added into different PBS (pH 7.4, 4.7 and 1.5) and incubated with cells for an additional 60 min at 37°C. The concentration of P,N-CD in the buffer solutions was controlled at 0.40 mg/mL. After that, the cells were washed three times in PBS (pH 7.4, 4.7 or 1.5) to remove excess P,N-CD. Fluorescence images were collected on a confocal laser scanning microscope.

In vivo zebrafish imaging

The zebrafish obtained from zebrafish core facility center, National Tsing Hua University, were used in all the experiments. All experiment were performed in compliance with the use of Regulation for Administration of Laboratory Animals. This is a regulation which was approved by the State Council and promulgated by State Ministry of Science and Technology in 1988, China. *In vivo* imaging was carried out with a multispectral fluorescent vivo molecular imaging system (S-0010A). The zebrafish was put in an aqueous solution containing P,N-CD (2.0 mg/mL). After different time intervals, the zebrafish was thoroughly rinsed with distilled water and imaged on the *in vivo* imaging system. Spectral fluorescence images were obtained using the appropriate filters for P,N-CD (excitation: 435 or 470 nm; emission: 525 or 570 nm long-pass filter; acquisition settings: 500–750 nm in 10 nm steps). Exposure times were automatically calculated and the acquisition setting was 1500 ms.

Results and discussion

To diagnostic detection and in many other areas, the main challenge in fluorescence-based analysis is to generalise the use of a common source which is widely available.[23] The objective of this study was to introduce a widely available natural product as a source to obtain P,N-CD. Here, we used the natural product, pumpkin to synthesise P,N-CD with yellow fluorescence emission.

The synthesis of P,N-CD was performed according to the acidic oxidation with pumpkin as the carbon source and H_3PO_4 as the oxidizing agent which was similar to carbonisation of ascorbic acid at 90°C.[47] Fig. 1 displays the general scheme to illustrate the synthesis of P,N-CD. The formation mechanisms of our P,N-CD based on the previous work of heteroatoms doped CD from small molecules[48,49] are postulated as: (1) hydrolysis, dehydration and fragmentation of small molecules, (2) polymerisation of the products formed in step1 and aromatisation of the polymers, (3) nucleation and growth of carbon substances, and (4) oxidation of grown carbon substances.

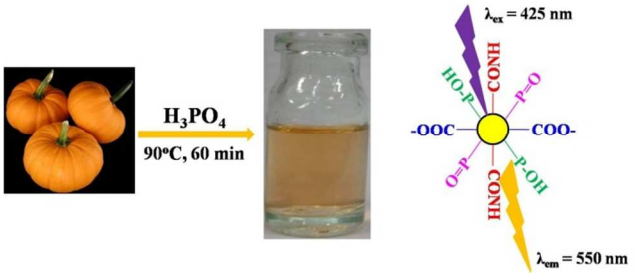

Fig. 1. Scheme illustrates the synthesis of phosphorus and nitrogen co-doped carbon dots.

Fig. 2a depicts the size distribution and morphology of the P,N-CD characterised by TEM. The P,N-CD are quasispherical and monodisperse with a narrow size distribution with the statistical diameters in the range of 3.75 ± 0.20 nm. The size distribution of the P,N-CD agrees well with the Gaussian distribution and the full width half maximum of the fitted curve is 1.05 nm, which further confirms the narrow size distribution of the as-prepared P,N-CD.

To probe the chemical composition and content of the as-synthesised P,N-CD, the elemental analysis and XPS measurements were obtained. Table S1A† summarises the elemental analysis of P,N-CD which is consistent with the results of XPS (*vide infra*). The doping concentrations of P and O are about 21.60 and 65.50% respectively which are much higher than those reported in the literature.[42,48] The elemental contents are expressed in terms of relative number of atom as depicted in Table S1B†. The empirical formula for P,N-CD is approximately $C_{13}H_{49}N_2P_{13}O_{74}$. Fig. 2b shows the survey XPS scan of P,N-CD sample, revealing the presence of C, N, O, and P as well as limited H without any other impurities. The binding energy peaks at 131.5, 190.0, 285.0, 398.2, and 531.0 eV correspond to P2p, P2s, C1s, N1s, and O1s, respectively. Therefore, the P,N-CD can be temporarily thought as phosphorus and nitrogen functionalised. Fig. 2c displays the high-resolved C1s spectrum which can be deconvoluted into six peaks at 284.8, 285.3, 286.0, 286.34, 287.4, and 288.2 eV, representing C1s states in C–C, C–OH/C–O–C, C–N, C=N, C=O, and COOH bonds, respectively.[42,48,50-52] The N1s spectrum (Fig. S1a†) shows three peaks at 399.7, 399.9 and 400.3 eV which are associated with C–N–C, pyrrolic-like N and N-$(C)_3$ functionalities, respectively.[51,52] The O1s of P,N-CD spectrum (Fig. S1b†) are deconvoluted into four peaks at 531.2, 531.5, 532.1, and 532.93 eV, which are attributed to O=C–O, P=O, C–OH/C–O–C, and O=C–O, respectively.[51,52] The high resolution P2p peak in Fig. 2d shows the P–C-binding motifs of the P,N-CD. The P2p peaks at about 134.4 and 133.6 eV indicate the phosphorus species to be tetra-coordinated phosphorous(V).[46,48,53] The phosphate, PO_4^{3-}, is modified on the surface of graphite core of P,N-CD by bidentate bonding, with C–OP=$O(OH)_2$ as the surface ends.[54] The phosphate on the P,N-CD may be derived from the thermal dehydration of hydroxyl phosphate moieties between –OH on the surface of carbon core and –P=O (OH) of the H_3PO_4.

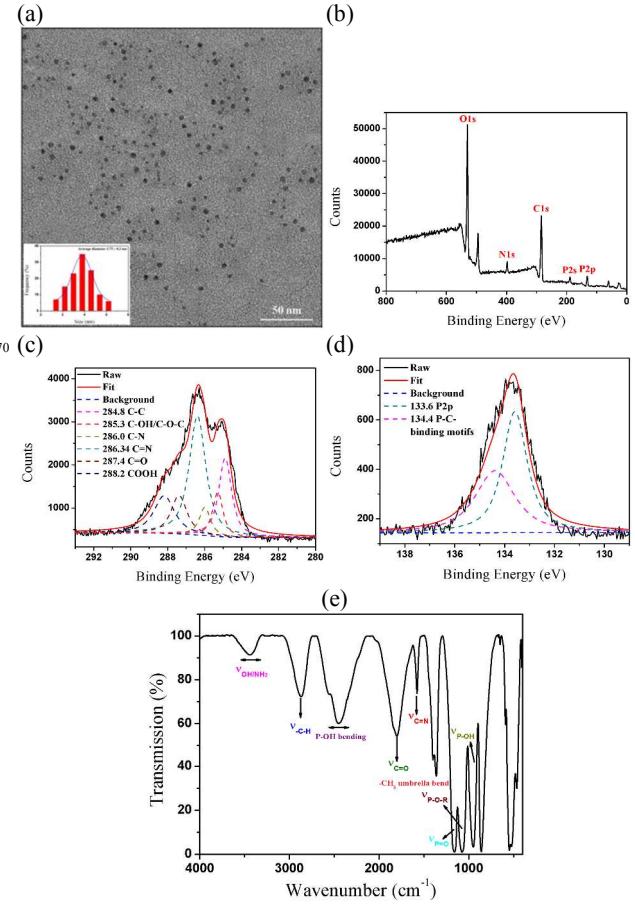

Fig. 2. (a) TEM image and particle size distribution (bottom inset) of the as-synthesised P,N-CD. (b) XPS survey scan of P,N-CD. (c) C1s XPS and (d) P2p XPS of P,N-CD. (e) FTIR spectrum of P,N-CD.

Fig. 2e displays the FTIR of P,N-CD. The existence of a broad peak centred at 3440 cm^{-1} represents the stretching vibrations of O–H or N–H bonds.[51,55] Several sharp peaks at 1360, 1576, 1780, and 2869 cm^{-1} corresponding to $–CH_3$ umbrella bend, C=N, C=O stretching, and –CH, respectively.[51,55] They can be assigned to phosphorus and phosphocarbonaceous moieties in the phosphoric acid activated carbons.[56] A broad peak between 3250 and 2500 cm^{-1}, corresponding to the P–OH bending of phosphate is observed, indicating that P,N-CD contains surface-attached phosphate moiety. Peaks at 1160, 1075 and 950 cm^{-1} are related to the stretching vibration of hydrogen-bonded P=O groups from phosphates or polyphosphates, $P–O–C_{(aromatic)}$ and P–O–H, respectively.[48,55,57] The functional groups identified by the FTIR are in good agreement with XPS, illustrating that the surface of P,N-CD is functionalised with phosphoric groups.

In quest of exploring the optical properties of the as-prepared P,N-CD, the UV-vis absorption and PL spectra were acquired and depicted in Fig. 3. As shown in the UV-vis absorption spectrum

(black line in Fig. 3a), we propose that the strong absorption peak of P,N-CD at 283 nm is corresponding to the $n\rightarrow\pi^*$ transition of C=O bond and the weak absorption peak at 228 nm is attributing to the $\pi\rightarrow\pi^*$ transition of aromatic sp^2 bond.[47] The PL spectra of P,N-CD are shown in Fig. 3a (red and blue lines). It can be seen that the optimal excitation (λ_{ex}) and emission (λ_{em}) wavelengths are located at 425 and 550 nm, respectively. The photograph of the P,N-CD dispersion under UV light (365 nm) exhibits strong yellow emission (inset of Fig. 3a).

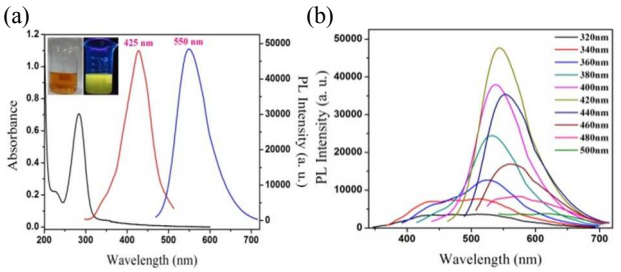

Fig. 3. (a) UV-vis absorption, PL excitation (λ_{ex}) and emission spectra of P,N-CD. The inset displays photographs of the P,N-CD under daylight (left) and UV irradiation (right) in aqueous solution. (b) PL spectra of P,N-CD at different λ_{ex} 320–500 nm. The concentration of P,N-CD is 0.20 mg/mL.

To further explore the optical properties of the as-prepared P,N-CD, the λ_{ex}-dependent PL behaviour was conducted and depicted in Fig. 3b. The PL spectra are bathochromically shifted with the increase in the λ_{ex}, indicating that the PL band can be tuned by adjusting the λ_{ex}. The λ_{em} are red-shifted from 439 to 636 nm for the P,N-CD when the λ_{ex} moves from 320 to 500 nm. The λ_{ex}-dependent PL behaviour is common with carbon dots.[27,28,51,52] This behaviour is contributed to the surface state affecting the band gap of CD. The surface state is analogous to a molecular state whereas the size effect is a result of quantum dimensions, both of which contribute to the complexity of the excited states of CD.[58] The λ_{ex}-dependent PL behaviour is useful for multicolour imaging applications (*vide infra*). Furthermore, using quinine sulfate (Fig. S2a†) as a reference, the fluorescence Φ_s of the as-synthesised P,N-CD (Fig. S2b†) was measured to be 9.42 %. The as-prepared P,N-CD exhibits excellent stability which is essential for practical applications. The effect of the ionic strength in terms of concentration of KCl on the PL stability of the P,N-CD was investigated. No significant changes in PL intensity or peak characteristics under different concentrations of KCl (Fig. S3†) was observed which is important because it is necessary for P,N-CD to be used in the presence of physical salt conditions in practical applications.

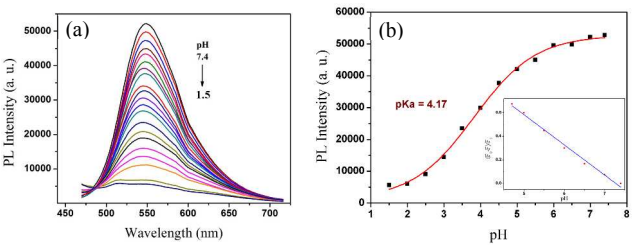

Fig. 4. (a) The PL spectra of 0.20 mg/mL P,N-CD as pH decreases from 7.4 to 1.5 at λ_{ex} of 425 nm. (b) The relationship between the PL intensity at $\lambda_{ex}/\lambda_{em}$ of 425/550 nm and pH. The inset displays the linear plot of $(F_0–F)/F_0$ against pH (4.7–7.4).

As pH plays a pivotal role in many chemical and biological systems, its detection is of critical importance. Fig. 4a depicts the change in PL spectra of P,N-CD at a broad pH range of 1.5–7.4 under λ_{ex} of 425 nm. The PL intensity decreases as pH decreases. The PL intensity can be related to the protonation and deprotonation of the P,N-CD.[59-62] When pH increases from 1.5 to 7.4, the carboxylic acid moieties on the surface of P,N-CD are deprotonated to carboxylates and then a negative charged "protective shell" is formed on the surface of P,N-CD which lowers the non-radiative recombination rate of the photo-excited state of P,N-CD;[63,64] consequently enhancing the PL intensity. This optically pH-sensitive property renders the P,N-CD as an attractive fluorescent probe for pH-monitoring in biological and biomedical applications. The PL spectra of P,N-CD at pH 1.0–14 is depicted in Fig. S4†.

Fig. 4b displays the plot of PL intensity against pH (1.5–7.4). A well fitted sigmoidal curve using the Boltzmann equation is obtained. The near-neutral pH range is investigated since the normal physiological hydrogen ion concentration varies within narrow limits and P,N-CD can be used to achieve the expected goal. Interestingly, a good linear relationship between PL intensity and pH (4.7–7.4) is found based on: $(F_0–F)/F_0 = 1.362–0.299\text{pH}$, $r^2 = 0.991$, where F_0 and F are the PL intensities of the P,N-CD at pH 7.4 and other pHs, respectively (inset of Fig. 4b). The pK_a of 4.17 ± 0.07 and the slope of 4.78 ± 0.13 were obtained by fitting the PL intensity with the Henderson-Hasselbalch equation. These results indicate that the P,N-CD can be applied to detect the intracellular pH quantitatively within the near neutrality range. In addition, the stability of this pH probe was tested by measuring the PL response for 200 min.

Fig. S5a† shows the time course of fluorescence intensity of the pH sensor at pH 7.4, 4.7 and 1.5 on exposure to a 75 W xenon arc lamp. The PL intensity is continuously monitored and recorded. The results indicate that the pH probe can instantly response to the change of H^+ concentration and the probe solution possesses good photostability. Thus, the probe can be used to real-time monitor pH. Furthermore, it is well-known that reversibility is highly desirable for monitoring pH changes in living organs. The pH of the solution is switched back and forth between 7.4 and 4.7 by using aqueous NaOH and HCl solutions. Fig. S5b† clearly reveals that the PL intensities are fully reversible. The response and recovery times in different pH solutions are rapid and within seconds.

The application of P,N-CD as a new fluorescent marker for *in vivo* and *in vitro* imaging was explored. For effective bioimaging, it is required that the selected fluorescent marker has not only optical merits but also low cytotoxicity. To evaluate the cytotoxicity of the P,N-CD, the viability of human breast adenocarcinoma MCF-7 cells treated with P,N-CD was measured by the MTT method. Fig. S6† shows MCF-7 cells incubated with different doses of P,N-CD for 24 and 48 h. The viability remained greater than 88.6% even incubated with ultrahigh concentration (400 μg/mL) of P,N-CD for 48 h, demonstrating low toxicity of the P,N-CD (without any further functionalisation) and inferring their potential use *in vivo* and *in vitro* imaging.

Given the low cytotoxicity, we further tested the toxicity and feasibility of P,N-CD as bioimaging agents in animals. The potential use of P,N-CD as luminescent probes for *in vivo* imaging was carried out on zebrafish. Zebrafish was placed in an aqueous solution containing 2.0 mg/mL P,N-CD at 23°C for 0.0–120 min and the images were taken under bright field and $\lambda_{ex}/\lambda_{em}$ of 470/570 nm as depicted in Fig. 5(a)–(e) and (f)–(j), respectively. No abnormal morphology was found for the zebrafish after exposure to P,N-CD for 120 min. The zebrafish still survive after the experiment.

Fig. S7† shows the λ_{ex}-dependent fluorescence image of zebrafish at $\lambda_{ex}/\lambda_{em}$ of 435/525 nm (green) and 470/570 nm

(yellow). Under a multispectral fluorescent vivo molecular imaging system, the head, stomach and tail of zebrafish exhibit strong characteristic yellow luminescence from P,N-CD (Fig. 5(g)–(j)), illustrating that P,N-CD could permeate throughout the animal cells and had no perceptible effect on animals. The fluorescence intensity of the zebrafish increases gradually with the increase in the exposure time to P,N-CD and reaches the highest at about 60 min. These results suggest that the P,N-CD without the modifier/surface passivated agent can stain zebrafish easily and show no obvious toxicity.

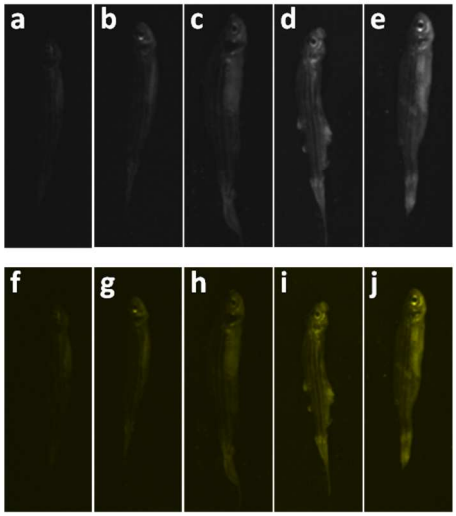

Fig. 5. *In vivo* zebrafish imaging of P,N-CD under bright field for (a) 0.0, (b) 15, (c) 30, (d) 60, and (e) 120 min. *In vivo* zebrafish imaging of P,N-CD under $\lambda_{ex}/\lambda_{em}$ of 470/570 nm for (f) 0.0, (g) 15, (h) 30, (i) 60, and (j) 120 min.

In order to explore the potential application of P,N-CD for *in vitro* imaging of living cells, MCF-7 cells were exposed to P,N-CD aqueous solutions at pH 7.4, 4.7 and 1.5 as shown in Fig. 6. The cells stained with P,N-CD display strongest yellow emissions at pH 7.4 (Fig. 6A and G). P,N-CD were well-dispersed in the cytoplasm region between the nucleus and the cell membrane. When the pH decreases to 4.7, the yellow emissions decrease (Fig. 6B and H). When the pH drops to 1.5, it is hardly found the yellow emissions (Fig. 6C and I). However, when the pH switches back to 7.4, the yellow emission is recovered, demonstrating the reversibility of emission of P,N-CD in the cells. Fig. 6(J) displays the intracellular fluorescence intensities of P,N-CD at pH 7.4, 4.7 and 1.5. The intensities of 28 cells in the red circle lines were measured. $\lambda_{ex}/\lambda_{em}$ are 515/570 ± 25 nm. It is obvious that the cells show the emission intensity at pH 7.4 > 4.7 > 1.5. Fig. S8† depicts the λ_{ex}-dependent fluorescence of the P,N-CD-stained cells at pH 7.4, 4.7 and 1.5. The cells display blue, green, yellow and red emissions at λ_{ex} of 405, 488, 515, and 543 nm, respectively. Again, the cells intensity follows at pH 7.4 > 4.7 > 1.5. These results further demonstrate that P,N-CD is an efficient fluorescent pH probe for reversibly monitoring the pH in live cells.

Conclusion

For the first time, P,N-CD has been synthesised from a fast, simple and "green" route with pumpkin as the carbon source and H_3PO_4 as the oxidation agent at low temperature (90°C). The morphology and chemical structures have been investigated extensively by TEM, XPS, FTIR, UV-vis absorption, and PL spectroscopy. The as-synthesised P,N-CD shows strong and stable PL which is dependent on λ_{ex}. Moreover, P,N-CD displays pH-dependent behaviour. The PL intensity is very strong at pH 7.4 but very weak at pH 1.5. P,N-CD also shares some other desired properties such as high fluorescence Φ_s, yellow emission, large Stokes shift, good reversibility, excellent photostability and cell membrane permeability. Since the P,N-CD hold these perfect properties and ultra-low toxicity, empowering their use in *in vitro* and *in vivo* cells imaging. It can be applied as an emission fluorescent probe to noninvasively monitor physiological pH in living cells. It is anticipated that P,N-CD is a promising candidate for real-time tracking of the intracellular pH especially under physiological conditions in the disease diagnosis, biosensors, biomedical and biological fields.

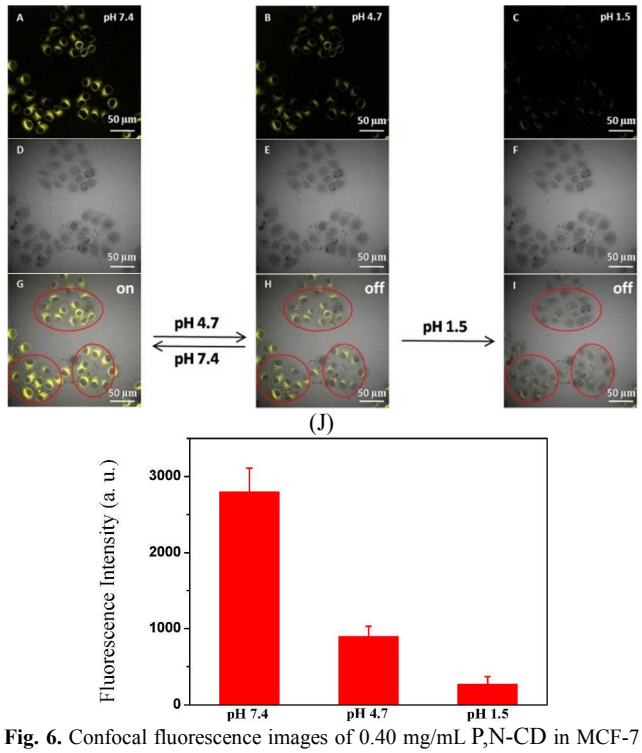

Fig. 6. Confocal fluorescence images of 0.40 mg/mL P,N-CD in MCF-7 cells at pH (A) 7.4, (B) 4.7 and (C) 1.5. (D) Bright field image, and (G) merged image of A and D at pH 7.4. (E) Bright field image, and (H) merged image of (B) and (E) at pH 4.7. (F) Bright field image, and (I) merged image of (C) and (F) at pH 1.4. (J) Intracellular fluorescence intensities of P,N-CD at pH 7.4, 4.7 and 1.5. Data are expressed as mean ± standard deviation. The intensities of 28 cells in the red circle lines were measured. $\lambda_{ex}/\lambda_{em}$ are 515/570 ± 25 nm.

Acknowledgements

This work was supported by the National Natural Science Foundation of China (21175086, 21405099 and 21175087).

Notes and references

[a]*Institute of Environmental Science, and School of Chemistry and Chemical Engineering, Shanxi University, Taiyuan 030006, China. Fax: +86-351-7018613; Tel: +86-351-7018613; E-mail: dc@sxu.edu.cn*
[b]*Partner State Key Laboratory of Environmental and Biological Analysis, and Department of Chemistry, Hong Kong Baptist University, 224 Waterloo Road, Kowloon Tong, Hong Kong SAR, China. Fax: +852-34117348; E-mail: mmfchoi@gmail.com*
[1]*Present address: Acadia Divinity College, Acadia University, 15 University Avenue, Wolfville, Nova Scotia, B4P 2R6, Canada.*
‡*These authors contributed equally to this work.*

†Electronic Supplementary Information (ESI) available: elemental analysis, N1s and O1s XPS of P,N-CD, plots of integrated PL intensity against absorbance of P,N-CD and quinine sulfate, effect of ionic strength and pH on PL intensity of P,N-CD, the time-dependence of fluorescent intensity of P,N-CD, PL spectra of the P,N-CD at pH 1.0 – 14, cell cytotoxic effects, *in vivo* zebrafish imaging of P,N-CD, confocal fluorescence imaging of MCF-7 cells with 0.40 mg/mL P,N-CD for 60 min at pH 7.4, 4.7 and 1.5. See DOI: 10.1039/b000000x/

1 S. N. Baker and G. A. Baker, *Angew. Chem. Int. Ed.*, 2010, **49**, 6726.
2 H. Li, Z. Kang, Y. Liu and S.-T. Lee, *J. Mater. Chem.*, 2012, **22**, 24230.
3 L. Cao, X. Wang, M. J. Meziani, F. Lu, H. Wang, P. G. Luo, Y. Lin, B. A. Harruff, L. M. Veca, D. Murray, S.-Y. Xie and Y.-P. Sun, *J. Am. Chem. Soc.*, 2007, **129**, 11318.
4 S.-T. Yang, L. Cao, P. G. Luo, F. Lu, X. Wang, H. Wang, M. J. Meziani, Y. Liu, G. Qi and Y.-P. Sun, *J. Am. Chem. Soc.*, 2009, **131**, 11308.
5 P. G. Luo, S. Sahu, S.-T. Yang, S. K. Sonkar, J. Wang, H. Wang, G. E. LeCroy, L. Cao and Y.-P. Sun, *J. Mater. Chem. B*, 2013, **1**, 2116.
6 J. Tang, B. Kong, H. Wu, M. Xu, Y. Wang, Y. Wang, D. Zhao and G. Zheng, *Adv. Mater.*, 2013, **25**, 6569.
7 J. Wang, C. F. Wang and S. Chen, *Angew. Chem. Int. Ed.*, 2012, **51**, 9297.
8 S. Qu, X. Wang, Q. Lu, X. Liu and L. Wang, *Angew. Chem. Int. Ed.*, 2012, **51**, 12215.
9 S. Zhu, Q. Meng, L. Wang, J. Zhang, Y. Song, H. Jin, K. Zhang, H. Sun, H. Wang and B. Yang, *Angew. Chem. Int. Ed.*, 2013, **52**, 3953.
10 L. Zhou, Y. Lin, Z. Huang, J. Ren and X. Qu, *Chem. Commun.*, 2012, **48**, 1147.
11 Q. Qu, A. Zhu, X. Shao, G. Shi and Y. Tian, *Chem. Commun.*, 2012, **48**, 5473.
12 W. Lu, X. Qin, S. Liu, G. Chang, Y. Zhang, Y. Luo, A. M. Asiri, A. O. Al-Youbi and X. Sun, *Anal. Chem.*, 2012, **84**, 5351.
13 Y. Dong, G. Li, N. Zhou, R. Wang, Y. Chi and G. Chen, *Anal. Chem.*, 2012, **84**, 8378.
14 V. Gupta, N. Chaudhary, R. Srivastava, G. D. Sharma, R. Bhardwaj and S. Chand, *J. Am. Chem. Soc.*, 2011, **133**, 9960.
15 Y. Li, Y. Hu, Y. Zhao, G. Shi, L. Deng, Y. Hou and L. Qu, *Adv. Mater.*, 2011, **23**, 776.
16 L. Tang, R. Ji, X. Cao, J. Lin, H. Jiang, X. Li, K. S. Teng, C. M. Luk, S. Zeng, J. Hao and S. P. Lau, *ACS Nano*, 2012, **6**, 5102.
17 H. Li, X. He, Z. Kang, H. Huang, Y. Liu, J. Liu, S. Lian, C. H. A. Tsang, X. Yang and S.-Y. Lee, *Angew. Chem. Int. Ed.*, 2010, **49**, 4430.
18 L. Cao, S. Sahu, P. Anilkumar, C. E. Bunker, J. Xu, K. A. S. Fernando, P. Wang, E. A. Guliants, K. N. Tackett and Y.-P. Sun, *J. Am. Chem. Soc.*, 2011, **133**, 4754.
19 S. Zhuo, M, Shao and S.-T. Lee, *ACS Nano*, 2012, **6**, 1059.
20 Q.-L. Zhao, Z.-L. Zhang, B.-H. Huang, J. Peng, M. Zhang and D.-W. Pang, *Chem. Commun.*, 2008, **41**, 5116.
21 M. Zhang, L. Bai, W. Shang, W. Xie, H. Ma, Y. Fu, D. Fang, H. Sun, L. Fan, M. Han, C. Liu and S. Yang, *J. Mater. Chem.*, 2012, **22**, 7461.
22 D. Pan, J. Zhang, Z. Li, C. Wu, X. Yan and M. Wu, *Chem. Commun.*, 2010, **46**, 3681.
23 H. Liu, T. Ye and C. Mao, *Angew. Chem. Int. Ed.*, 2007, **46**, 6473.
24 Y. Yang, J. Cui, M. Zheng, C. Hu, S. Tan, Y. Xiao, Q. Yang and Y. Liu, *Chem. Commun.*, 2012, **48**, 380.
25 C. Zhu, J. Zhai and S. Dong, *Chem. Commun.*, 2012, **48**, 9367.
26 Q. Wang, H. Zheng, Y. Long, L. Zhang, M. Gao and W. Bai, *Carbon*, 2011, **49**, 3134.
27 X. Gong, W. Lu, M. C. Paau, Q. Hu, X. Wu, S. Shuang, C. Dong and M. M. F. Choi, *Anal. Chim. Acta*, 2015, **861**, 74.
28 W. Lu, X. Gong, Z. Yang, Y. Zhang, Q. Hu, S. Shuang, C. Dong and M. M. F. Choi, *RSC Adv.*, 2015, **5**, 16972.
29 Z. Ma, H. Ming, H. Huang, Y. Liu and Z. H. Kang, *New J. Chem.*, 2012, **36**, 861.
30 H. Li, X. He, Y. Liu, H. Huang, S. Lian, S.-T. Lee and Z. Kang, *Carbon*, 2011, **49**, 605.
31 L. Jiong, S. Pei, Y. Emmeline, G. C. Kwan, W. Ping and L. K. Ping, *Nat. Nanotechnol.*, 2011, **6**, 247.
32 X. Xu, R. Ray, Y. Gu, H. J. Ploehn, L. Gearheart, K. Raker and W. A. Scrivens, *J. Am. Chem. Soc.*, 2004, **126**, 12736.
33 S.-L. Hu, K.-Y. Niu, J. Sun, J. Yang, N.-Q. Zhao and X.-W. Du, *J. Mater. Chem.*, 2009, **19**, 484.
34 S. Yang, H. Zeng, H. Zhao, H. Zhang and W. Cai, *J. Mater. Chem.*, 2011, **21**, 4432.
35 H. Jiang, F. Chen, M. G. Lagally and F. S. Denes, *Langmuir*, 2010, **26**, 1991.
36 W. Kwon, J. Lim, J. Lee, T. Park and S.-W. Rhee, *J. Mater. Chem. C*, 2013, **1**, 2002.
37 Y. Dong, R. Wang, H. Li, J. Shao, Y. Chi, X. Lin and G. Chen, *Carbon*, 2012, **50**, 2810.
38 H. Zheng, Q. Wang, Y. Long, H. Zhang, X. Huang and R. Zhu, *Chem. Commun.*, 2011, **47**, 10650.
39 Y.-Q. Zhang, D.-K. Ma, Y. Zhuang, X. Zhang, W. Chen, L.-L. Hong, Q.-X. Yan, K. Yu and S.-M. Huang, *J. Mater. Chem.*, 2012, **22**, 16714.
40 Z. Qian, J. Ma, X. Shan, H. Feng, L. Shao and J. Chen, *Chem.-Eur. J.*, 2014, **20**, 2254.
41 S. Chandra, P. Das, S. Bag, D. Laha and P. Pramanik, *Nanoscale*, 2011, **3**, 1533.
42 N. K. Chaudhari, M. Y. Song and J.-S. Yu, *Sci. Rep.*, 2014, **4**, 5221.
43 D. H. Seo, A. E. Rider, S. Kumar, L. K. Randeniya and K. Ostrikov, *Carbon*, 2013, **60**, 221.
44 S. Sahu, B. Behera, T. K. Maiti and S. Mohapatra, *Chem. Commun.*, 2012, **48**, 8835.
45 C. Mattevi, G. Eda, S. Agnoli, S. Miller, K. A. Mkhoyan, O. Celik, D. Mastrogiovanni, G. Granozzi, E. Garfunkel and M. Chhowalla, *Adv. Funct. Mater.*, 2009, **19**, 2577.
46 J. P. Paraknowitsch, Y. Zhang, B. Wienert and A. Thomas, *Chem. Commun.*, 2013, **49**, 1208.
47 Z. Luo, Y. S. Lu, A. Luke and A. T. C. Johnson, *J. Am. Chem. Soc.*, 2009, **131**, 898.
48 Z.-Q. Xu, L.-Y. Yang, X.-Y. Fan, J.-C. Jin, J. Mei, W. Peng, F.-L. Jiang, Q. Xiao and Y. Liu, *Carbon*, 2014, **66**, 351.
49 H. Li, H. Ming, Y. Liu, H. Yu, X. He, H. Huang, K. Pan, Z. Kang and S.-Y. Lee, *New J. Chem.*, 2011, **35**, 2666.
50 Y.-C. Lu, J. Chen, A.-J. Wang, N. Bao, J.-J. Feng, W. Wang and L. Shao, *J. Mater. Chem. C*, 2015, **3**, 73.
51 X. Chen, Q. Jin, L. Wu, C. H. Tung and X. Tang, *Angew. Chem.*, 2014, **126**, 12750.
52 X. Jin, X. Sun, G. Chen, L. Ding, Y. Li, Z. Liu, Z. Wang, W. Pan, C. Hu and J. Wang, *Carbon*, 2015, **81**, 388.
53 D. Carriazo, M. C. Gutiérrez, F. Picó, J. M. Rojo, J. L. G. Fierro, M. L. Ferrer and F. Monte, *ChemSusChem*, 2012, **5**, 1405.
54 L. He, L. Jing, Z. Li, W. Sun and C. Liu, *RSC Adv.*, 2013, **3**, 7438.
55 X. Gong, Q. Hu, M. C. Paau, Y. Zhang, S. Shuang, C. Dong and M. M. F. Choi, *Nanoscale*, 2014, **6**, 8162.
56 P. Vinke, M. Van Der Eijk, M. Verbree, A. F. Voskamp and H. M. Van Bekkum, *Carbon*, 1994, **32**, 675.
57 A. M. Puziy, O. I. Poddubnaya, A. Martínez-Alonso, A. Castro-Muñíz, F. Suárez-García and J. M. D. Tascón, *Carbon*, 2007, **45**, 1941.
58 J. Shang, L. Ma, J. Li, W. Ai, T. Yu and G. G. Gurzadyan, *Sci. Rep.*, 2012, **2**, 792.
59 Y. Hu, J. Yang, J. Tian, L. Jia and J.-S. Yu, *Carbon*, 2014, **77**, 775.
60 C. Galande, A. D. Mohite, A. V. Naumov, W. Gao, L. Ci, A. Ajayan, H. Gao, A. Srivastava, R. B. Weisman and P. M. Ajayan, *Sci. Rep.*, 2011, **1**, 85.
61 X. Jia, J. Li and E. Wang, *Nanoscale*, 2012, **4**, 5572.
62 L. Shen, L. Zhang, M. Chen, X. Chen and J. Wang, *Carbon*, 2013, **55**, 343.
63 C. Zheng, X. An and J. Gong, *RSC Adv.*, 2015, **5**, 32319.
64 W. Kong, H. Wu, Z. Ye, R. Li, T. Xu and B. Zhang, *J. Lumin.*, 2014, **148**, 238.

Graphical Abstract

A simple and high-output strategy for the fabrication of yellow fluorescent phosphorous and nitrogen co-doped carbon dots (P,N-CD) is developed. The P,N-CD is biocompatible, has low toxicity, and shows distinctive photoluminescence properties. The P,N-CD is inexpensive to be synthesised and is potentially useful for versatile applications such as pH sensor, *in vitro* and *in vivo* imaging.